DOI:10.22059/IJVM.2024.374252.1005540 Iranian Journal of Veterinary Medicine Original Article

Online ISSN: 2252-0554`

Protective Effects of Eugenol Against Iron Overload-Induced Nephrotoxicity in Male Rats

Ahmed M. Malik Al-Mashhadi , Nabeel Mohammed Al-Sharafi

Department of Physiology, Biochemistry, and Pharmacology, Faculty of Veterinary Medicine University of Kufa, Kufa, Iraq.

Abstract

Background: Nephrotoxicity is the term used to describe when the renal system suffers from reduced renal function due to both direct and indirect toxin damage brought on by exposure to certain drugs.

Objectives: This study aimed to investigate. The protective effects of eugenol against nephrotoxicity induced by iron overload in male rats.

Methods: A total of 30 rats were randomly divided into six equal groups as follows: the 1st group controlled negative C- I.P injection of distilled water. The 2nd group, control positive C+, received iron dextran only at 100 mg/kg-BW I.P. The 3rd and 4th groups (IE1& IE2, respectively) received iron dextran 100 mg/kg-BW I.P and eugenol 50,100 mg/kg-BW orally, respectively, simultaneously. The 5th and 6th groups (E3& E4 respectively) received eugenol only at 50,100 mg/kg-BW orally.

Results: The study's findings revealed significant improvements in various biomarkers and histological characteristics in rats treated with eugenol compared to the control group (C+). Specifically, rats treated with eugenol exhibited decreased levels of creatinine, blood urea nitrogen (BUN), Malondialdehyde (MDA), Erythropoietin (EPO), and kidney injury molecule-1 (Kim-1), along with increased concentrations of Glutathione (GSH).

Microscopic examination of kidney tissue from control (C-) and eugenol-treated (E3 and E4) groups showed typical histological features, indicating preserved kidney architecture. In contrast, the control group (C+) displayed epithelial cell necrosis in renal tubules and inflammatory processes, particularly in glomeruli and the interstitial section of proximal renal tubules. The iron-exposed groups (IE1 and IE2) exhibited varying degrees of renal damage, with IE1 showing moderate epithelial cell necrosis and inflammation, while IE2 displayed relatively normal cortical architecture with mild inflammatory changes in the medulla.

Conclusion: The present study, in conclusion, eugenol has an ameliorative effect against iron overload-induced nephrotoxicity in male rats.

Keywords: Eugenol, Histopathology, Iron overload, Kidney Score, Nephrotoxicity

Introduction

Nephrotoxicity is when kidney damage experiences diminished efficiency due to direct or indirect toxin damage caused by exposure to certain medications in the renal system, frequently precipitating toxic effects (Sales and Foresto, 2020; Polaka *et al*., 2023). Since the kidney is the main organ responsible for eliminating xenobiotics, it is especially vulnerable to the detrimental impacts of drugs and their metabolites during excretion. Additionally, several medications exhibit a preference for nephrotoxicity, which raises the risk of kidney injury when administered (Sharma and Singh, 2023).

Iron overload (IOL) is well-acknowledged as a prevalent form of metal toxicity and is known to increase the risk of several acute and chronic diseases (Ige *et al*., 2019). IOL disorders include a range of illnesses characterized by elevated levels of iron throughout the body, which can cause damage to various organs such as the liver, kidney, heart, and spleen (Hsu *et al*., 2022 Seyednejad *et al*., 2023). Kidney illnesses are also affected by the toxic effects of iron, and ferroptosis is recognized as a pathophysiological mechanism that could be targeted therapeutically to prevent kidney damage or disease development. Ferroptosis is a form of cell death linked to oxidative stress caused by iron (Ríos-Silva *et al*., 2023). Several studies have associated iron overload with organ dysfunction and damage such as cardiac, hepatic, renal, and diabetic disease (Udan *et al*., 2019; Verna and Estuningtyas, 2022; Koohkan *et al*., 2023; Heriatmo *et al*., 2023).

Eugenol (EUG) is a weakly acidic phenolic of clove oil, comprising 83%–95% of the oil. It is slightly water-soluble and easily soluble in organic solvents, colorless or pale yellowish. The name is derived from the scientific name for clove, *Eugenia aromaticum*, or *Eugenia caryophyllid* (Dable-Tupas *et al*., 2023). EUG is a phenylpropanoid formally derived from guaiacol with an allyl chain substituted *para* to the hydroxy group. It is a significant component of clove essential oil and a natural compound used in traditional medicine. Several studies reported the healthy benefit effect of EUG in vivo and in vitro, the antioxidant, anti-inflammatory, neuroprotective, analgesic, and antibacterial properties (Ikawati *et al*., 2022; Shahsavari *et al*., 2023).

Eugenol has a protective effect making it a therapeutic agent for various chronic diseases that involve metabolic syndrome due to abnormalities in chronic kidney disease (Gharaei *et al*., 2022), renal toxicity induced by vitamin D (Elkhadragy *et al*., 2022), certain cancer diseases (Melo *et al*., 2023), and widely used in dentistry to treat toothache and pulpitis (Vilela *et al*., 2023).

Thus, our study was designed to evaluate the effects of eugenol against iron overload and induce nephrotoxicity.

Materials and Methods

Ethical Approval

This study was approved by the Scientific Committee of the Faculty of Veterinary Medicine, University of Kufa, and conforms to the ethical principles of care and Laboratory animals Approval number (UK.VET.2023/11/7.27151).

Experimental animals

Thirty albino rats, each weighing between 200 and 250 grams. The rats were housed in the animal facility of the Faculty of Veterinary Medicine, University of Kufa. The rats were housed in sterile plastic enclosures, with each cage accommodating five rats. Wood shavings were provided as bedding material. The animals were maintained at a regulated room temperature ranging from 23 to 25 °C, with a 12-hour alternating light and dark cycle and enough ventilation in the surroundings. The animals had two weeks of acclimation before the commencement of the trial. Ad libitum access to ordinary pellets and water was provided to them throughout the experiment.

Experimental design

The animals were randomly divided into six equal groups (n=5 for each) of treatment administrations during 30 experimental days. Control Negative Group (C-): Five healthy male rats were injected I.P. with distal water. Control Positive Group(C+): Five male rats received iron dextran (LYFEXT ®/USP/ India BN: ML22395) 100 mg/kg-BW I.P. injection every 72 hours. Group IE1**:** Five male rats received iron dextran 100 mg/kg-BW I.P. injection every 72 hours and orally gavages eugenol (Solarbio-China CN: 97-53-0) 50 mg/kg -BW per day. Group IE2**:** Five male rats received an iron dextran 100 mg/kg-BW I.P. injection every 72 hours and were given eugenol 100 mg/kg -BW daily. Group E3: Five male rats received orally eugenol 50 mg/kg -BW per day. Group E4**:** Five male rats received 100 mg/kg -BW of eugenol orally per day. After the end of the experiment, the animals were prepared for anesthetising using intramuscular injection of Ketamine 80 mg/kg B.W combined with Xylazine 8 mg /kg B.W (Jirkof and Lofgren, 2023).

Blood Sample Collection

Blood samples were collected via cardiac puncture technique using an EDTA tube. Serum was separated from the gel tube by centrifugation at (3000 rpm) for 15 minutes and stored

at -20 Cº (Abdul and Mlaghee, 2023) until use in the kidney function test, creatinine test (Biolabo- France REF: 80107), and blood urea nitrogen (MTD Diagnostic- Italy REF: CC1450) measurements using by Spectrophotometric according to (Wu and Tietz, 2006; Rifai, 2022). Oxidative status parameter GSH (Solarbio-China BC: 1170) and MDA (Solarbio-China BC: 0020) measurements using Spectrophotometric content according to (Alpert *et al*., 1985; Spitz *et al*., 1989). Serum EPO and KIM-1 levels were quantitatively measured using an enzyme-linked immunosorbent assay (ELISA) kit (BT LAB Kit- China CN: E0293Ra) and (BT LAB Kit- China CN: E0549Ra) by using an Elisa reader device (Stat fax -USA).

Histopathological Examination

Rats were placed to sleep, and the abdominal area was opened. Kidney tissue samples were taken. After sample collection, the tissue samples were removed and then fixed in 10% formalin for 24 hours. After the tissues were fixed, they were dehydrated by passing them through 70%, 80%, 90%, and 100% ethyl alcohol twice each for 2 hours, and then they were cleaned with xylene for 1/2 hour. Samples were filled with paraffin wax at 58–60 °C and then covered with more paraffin wax to make paraffin blocks. Using a rotary microtome, sliced to 0.5 cm thick, placed in plastic cassettes, stained using hematoxylin and eosin (H& E), and then looked at under a microscopic examination at 40x, 100x magnifications (Luna, 1968; Saleh mehdy Al-zeiny and Abbas, 2017). The cortex and medulla areas injured were evaluated by a scoring system divided into four scores shown in the Table (Jablonski, 1983).

Statistical analysis

The experimental data were statistically analyzed using Graph Pad Prism version 7. Tukey multiple comparisons and analysis of variance (ANOVA) were conducted to determine the significance of the variations among the groups. The data were presented as mean ± standard errors of the mean (SEM), with a statistically significant P value of less than 0.05 (Al-Sharafi and Al-Sharafi, 2014; Ntumi, 2021).

Results

The effects of iron dextran and eugenol administration on Biochemical serum concentration parameters treated male rats.

1- Serum creatinine concentration (mg/dL)

The effect of iron and different concentrations of eugenol on serum creatinine concentration (mg/dL) after 30 days of treatment. The control positive (C+) group, which received an injection of iron dextran 100 mg/kg body weight every 72 hours, exhibited a significant increase in serum creatinine concentration compared to all other groups ($P \geq 0.05$). Interestingly, there were no significant differences ($P \leq 0.05$) in serum creatinine concentration compared to each other among the eugenol-treated groups illustrated in Figure 1.

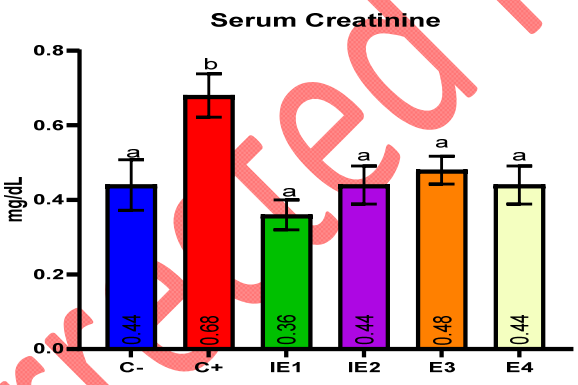

Figure (1): The effect of eugenol and iron dextran injection on serum Creatinine concentration (mg/dL) in male rats. The different letters explained the significant differences among groups, while the similar letters denote non-significant differences among groups. The error bars explain mean ± SEM for p-value at ($p \geq 0.05$); ANOVA one-way statistical analysis was used to calculate the significance differences among groups.

2- Serum blood urea nitrogen concentration (mg/dL)

The mean values of serum blood urea nitrogen (BUN) concentration (mg/dL) in the control group and the groups treated with iron and different concentrations of eugenol throughout the experimental period. The results demonstrate a significant increase ($P \geq 0.05$) in

BUN concentration in the control positive (C+) group, which received iron dextran injections, compared to all experimental groups. Furthermore, the findings reveal significant differences between the eugenol groups since the IE1 group (iron dextran + eugenol 50 mg/kg body weight) exhibited a significantly lower BUN concentration compared to all other eugenol groups (IE2, E3, and E4). However, the BUN concentration in the IE1 group was non-significantly different from that of the control negative group depicted in (Figure 2).

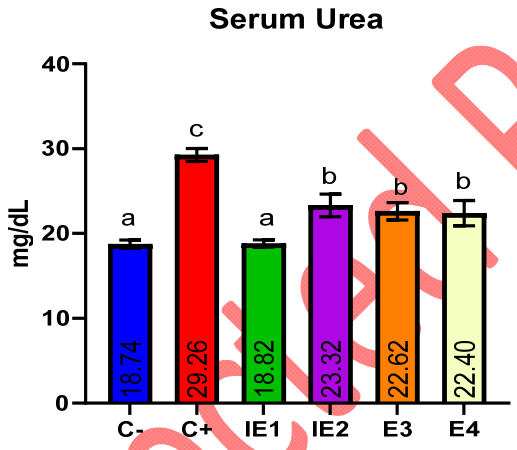

Figure (2): the effect of eugenol and iron dextran injection on serum BUN concentration (mg/dL) in male rats. The different letters explained the significance differences among groups, while the similar letters denote non-significant differences among groups. The error bars explain mean ± SEM for p-value at ($p \geq 0.05$); ANOVA one-way statistical analysis was used to calculate the significance differences among groups.

The effects of iron dextran and eugenol administration on some Oxidative status parameters in nephrotoxicity by iron overload treated male rats.

1- Detection of serum-reduced Glutathione concentration (GSH) µg /ml

(Figure 3) showed the concentration of GSH (µg/mL) in male rats belonging to the control group and the groups treated with iron and varying concentrations of eugenol throughout

the experimental period. The results indicate a significant decrease ($P \leq 0.05$) in GSH concentration in the control positive (C+) group compared to all experimental groups. Further analysis of the eugenol groups revealed a significantly lower GSH concentration in the IE2 (iron dextran + eugenol 100 mg/kg body weight) group compared to all other groups. Conversely, the GSH concentration in the E4 (eugenol 100 mg/kg body weight) group was significantly higher than all other groups. Interestingly, the GSH concentrations in the IE1 and E3 (eugenol 50 mg/kg body weight) groups were not significantly different. Notably, the GSH concentration in the control negative (C-) group was not significantly different from the IE1, IE2, and E3 groups. However, the GSH concentration in the control negative group was considerably lower than in the E4 group.

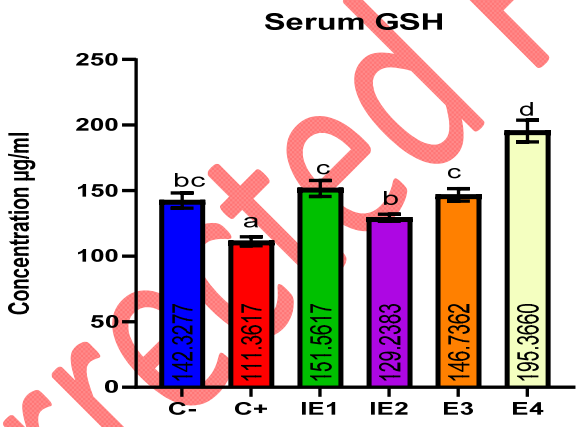

Figure (3): The effect of eugenol and iron dextran injection on kidney serum reduced Glutathione concentration (GSH) µg /ml in male rats. The different letters explained the significant differences among groups, while the similar letters denote non-significant differences among groups. The error bars explain mean ± SEM for p-value at ($p \geq 0.05$); ANOVA one-way statistical analysis was used to calculate the significance differences among groups.

2- Detection of serum Malondialdehyde concentration (MDA) nmol /mL

(Figure 4) illustrates the concentration of MDA (mmol/mL) in male rats of the control group and the groups treated with iron and varying concentrations of eugenol throughout the

experimental period. The results demonstrate a significant elevation ($P \geq 0.05$) in serum MDA concentration in the control positive (C+) group compared to all experimental groups. Further analysis of the iron + eugenol treated groups (IE1 and IE2) showed a non-significant difference ($P \leq 0.05$) in MDA concentration between the two groups. However, the MDA concentration in the IE1 group was significantly lower compared to the E4 group. Interestingly, there was a non-significant difference in MDA concentration between the IE2, E3, and E4 groups. Additionally, the MDA concentration in the control negative (C-) group was significantly lower than in all other groups except IE1.

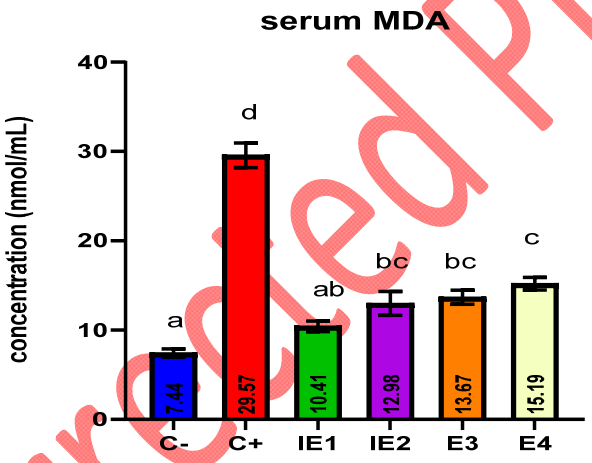

Figure (4): The effect of eugenol and iron dextran injection on kidney serum Malondialdehyde concentration (MDA) nmol /mL in male rats. The different letters explained the significant differences among groups, while the similar letters denote non-significant differences among groups. The error bars explain mean ± SEM for p-value at ($p \geq 0.05$); ANOVA one-way statistical analysis was used to calculate the significance differences among groups.

The effects of iron dextran and eugenol administration on ELISA Assay parameters in nephrotoxicity by iron overload treated male rats.

1- Serum Erythropoietin concentration pg/ml

The results from (Figure 5) elucidate the impact of iron dextran injection and daily oral eugenol administration on serum erythropoietin (EPO) concentration (pg/ml) in male albino rats. The findings showed a non-significant difference in serum EPO levels between the C+ E3 and E4 groups. However, a significant reduction ($P \geq 0.05$) was observed in the IE1, IE2, and C- groups compared to the C+ group. Interestingly, a non-significant difference in serum EPO levels was detected between the IE1 and IE2 groups. Nonetheless, both IE1 and IE2 groups exhibited significantly lower serum EPO levels than the E3 and E4 groups. Notably, the E4 group demonstrated the highest serum EPO levels. Additionally, a significant decrease in serum EPO levels was observed in the C- group relative to all eugenol-treated groups.

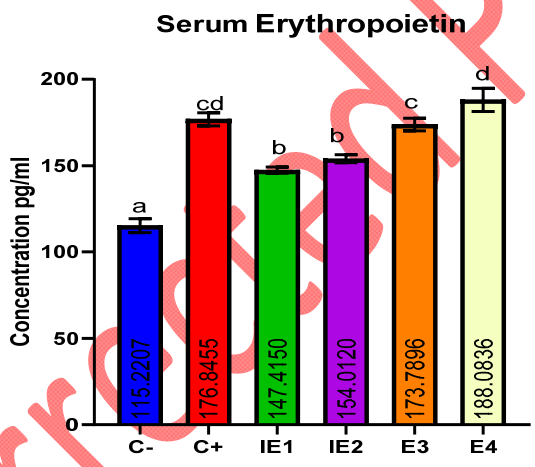

Figure (5): The effect of eugenol orally and iron dextran injection on serum Erythropoietin concentration pg/ml in male albino rats. The different letters explained the significant differences among groups, while the similar letters denote non-significant differences among groups. The error bars explain mean ± SEM for p-value at ($p \geq 0.05$); ANOVA one-way statistical analysis was used to calculate the significance differences among groups.

2- Serum Kidney Injury Molecule-1concentration ng/ml

(Figure 6) showed the impact of iron dextran injection and daily oral eugenol administration on KIM-1 levels in male albino rats. The results demonstrate a significant increase ($P \geq 0.05$) in

KIM-1 concentration in the C+ group compared to all experimental groups. Additionally, the IE2 group exhibited a notable decrease in KIM-1 levels compared to the IE1 and E4 groups while maintaining a non-significant difference from the E3 group. Furthermore, no significant differences were observed among the eugenol-treated groups (IE1, E3, and E4) or between the C- and IE2 groups.

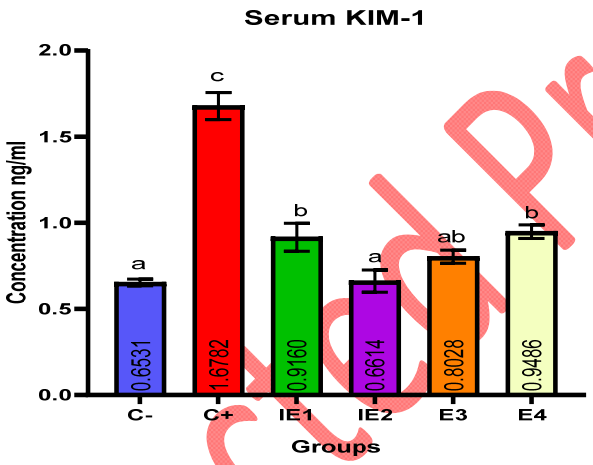

Figure (6): The effect of eugenol orally and iron dextran injection on serum KIM-1 concentration in male albino rats. The different letters explained the significant differences among groups, while the similar letters denote non-significant differences among groups. The error bars explain mean ± SEM for p-value at ($p \geq 0.05$); ANOVA one-way statistical analysis was used to calculate the significance differences among groups.

Microscopic examination

The microscopic examination of kidney rats in the control negative group (C-) did not show any histological changes in kidney tissue (Figure-7. A, B), and eugenol 50 and eugenol 100 (E3, E4) treated groups showed typical histological architecture of the kidney (Figure-8, 9. A, B). Rat kidneys of control positive groups (C+) showed necrosis of epithelial cells of proximal and distal convoluted tubules, leading to spaces in the cortex area. Also, infiltration of inflammatory cells in the affected cortex area filled the necrotic spaces (Figure-10. A, B). In the medulla, changes in necrosis of epithelial cells of the loop of Henle tubules led to space in the

medulla area where inflammatory cells aggregated to form a cluster that occupied the necrotic cells' spaces in spaces of necrotic tissue (Figure-11. A, B).

Rat kidney of iron dextran and eugenol at 50 mg/kg body weight (IE1). Showed moderate necrosis of epithelial cells of proximal and distal convoluted renal tubules led to from space in cortex area. Also, aggregation of infiltration of inflammatory cells in spaces of necrotic tissue (Figure-12. A, B) and in the medulla histological changes Moderate infiltration of inflammatory cell with presences of necrosis in epithelial cell of renal tubules of the loop of Henle of medulla area (Figure-13. A, B). Finally, the rat kidney of iron dextran and eugenol at a dosage of 100 mg/kg body weight (IE2) showed Normal histological architecture of the proximal and distal convoluted tubules of the cortex area of the kidney (Figure-14. A, B) and in the medulla mild infiltration of inflammatory cell between medullary renal tubules of the loop of Henle (Figure-15. A, B).

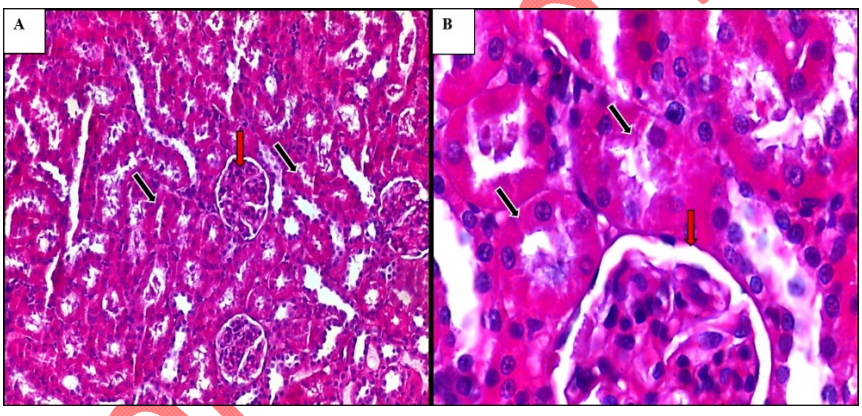

Figure (7 A and B): Photomicrograph of kidney of Control negative group rat. A&B/ Normal histological architecture of kidney. Note the glomerulus (red arrow) and convoluted tubules (black arrow). **H&E. A: 100x and B: 400x**.

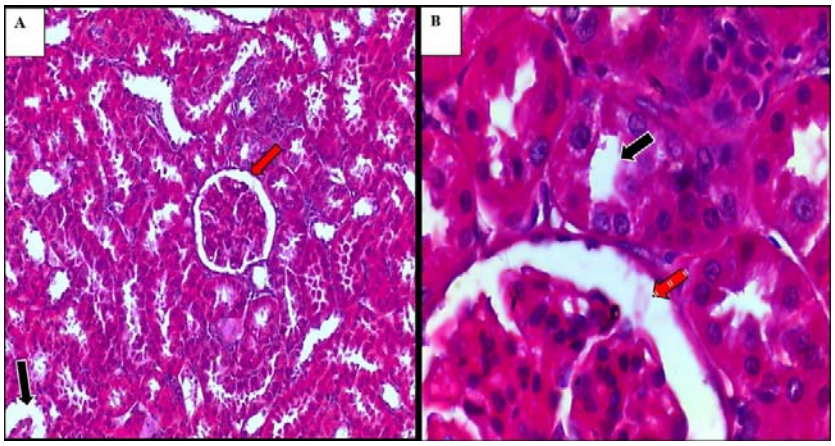

Figure (8 A and B): Photomicrograph of kidney of eugenol 50 (E3) group rat. A&B/ Normal histological architecture of kidney. Note the glomerulus (red arrow) and convoluted tubules (black arrow). H&E. A: 100x and B: 400x.

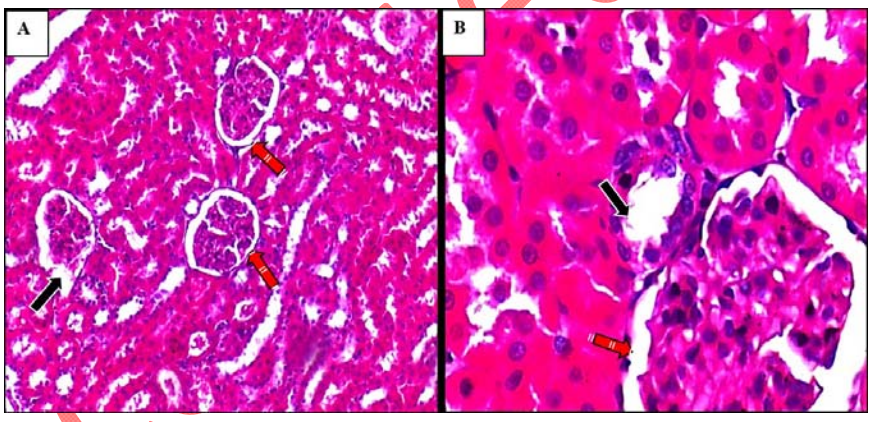

Figure (9 A and B): Photomicrograph of eugenol 100 (E4) group rat kidney. A&B/ Normal histological architecture of kidney. Note the glomerulus (red arrow) and convoluted tubules (black arrow). H&E. A: 100x and B: 400x.

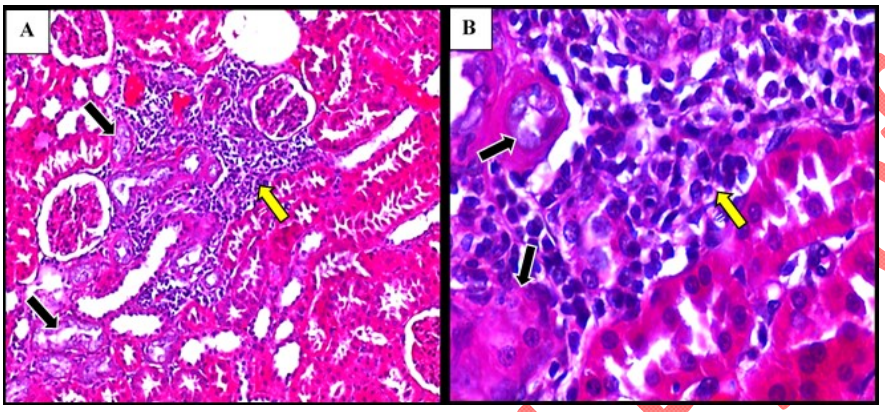

Figure (10 A and B): **Photomicrograph cortex area of kidney of control positive group rat**. A&B/ Necrosis of epithelial cells of proximal & distal convoluted tubules (black arrow) led to spaces in the cortex area. Also, infiltration of the inflammatory cell (yellow arrow) in the affected cortex area filled the necrotic spaces.

H &E. A: 100x and B: 400x.

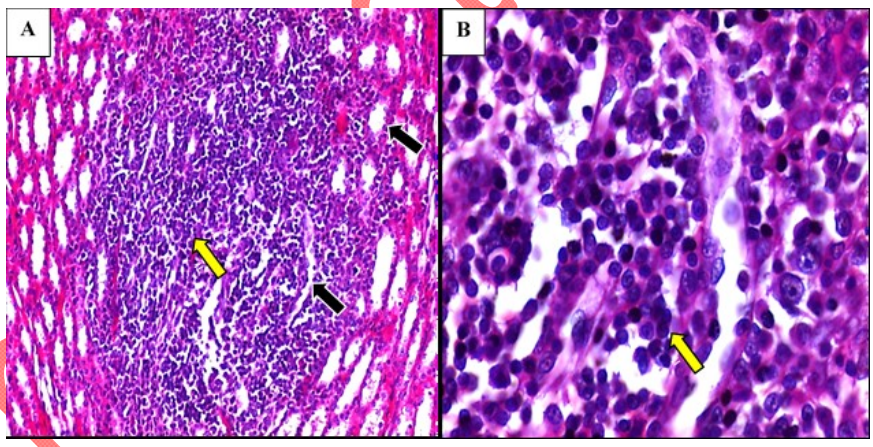

Figure (11 A and B): Photomicrograph medulla area of kidney of control positive group rat. A&B/ Necrosis of epithelial cells of renal tubules (black arrow) led to space in the medulla area where inflammatory cells

aggregated (yellow arrow) to form a cluster that occupied the necrotic cells' spaces in spaces of necrotic tissue. **H&E. A: 100x and B: 400x.**

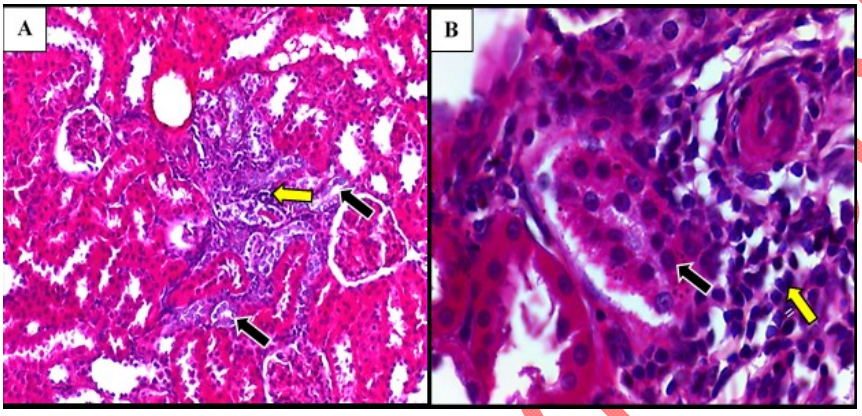

Figure (12 A and B): Photomicrograph cortex area of kidney of IE1 group rat. A&B/ Moderate Necrosis of epithelial cells of proximal and distal convoluted renal tubules (black arrow) led to from space in cortex area. Aggregation of infiltration of inflammatory cells (yellow arrow) in spaces of necrotic tissue. **H&E. A: 100x and B: 400x.**

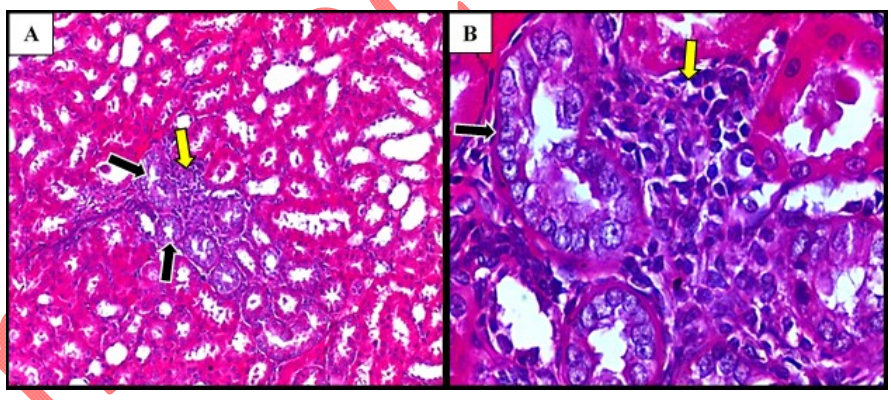

Figure (13 A and B): ***Photomicrograph medulla area of kidney of IE1 group rat.*** *A&B/ Moderate infiltration of the inflammatory cell (yellow arrow) with necrosis in epithelial cells of renal tubules (black arrow) of the loop of Henle of the medulla area.* ***H&E. A: 100x and B: 400x.***

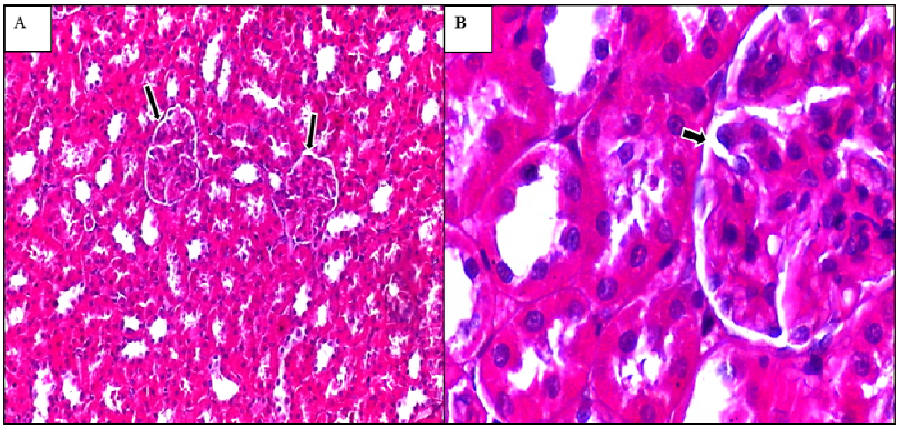

Figure (14 A and B): Photomicrograph cortex area of kidney of IE2 group rat. A&B/ Normal histological architecture of proximal & distal of convoluted tubules (black arrow) of cortex area of kidney. **H&E. A: 100x and B: 400x**.

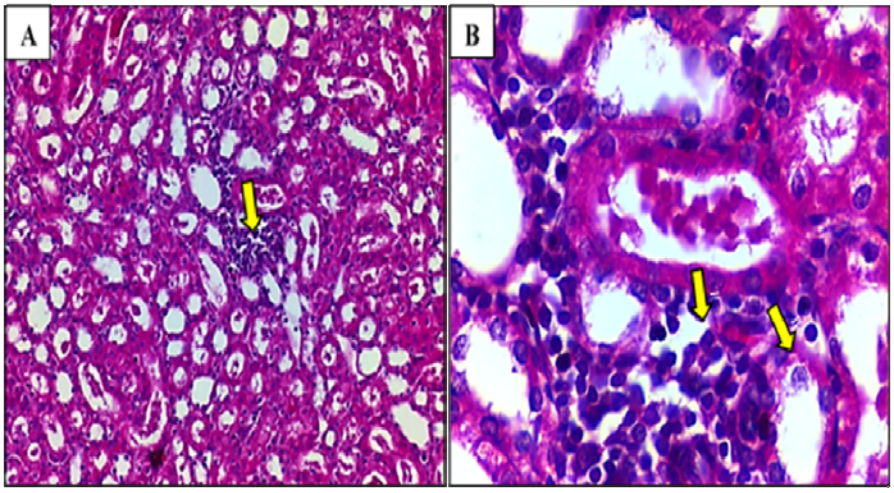

Figure (15 A and B): Photomicrograph medulla area of kidney of IE2 group rat. A&B/ Mild infiltration of the inflammatory cell (yellow arrow) between medullary renal tubules of the loop of Henle. **H&E. A: 100x and B: 400x.**

Kidney Injury Score

According to the Jablonski renal damage score system, the results show different grades of injury in the renal tissue for rats. There was a significant increase in the renal damage score ($P \geq 0.05$) for the cortex and medulla in the C+ group compared with other experiment groups. However, there were non-significant changes between IE1 and IE2 groups; otherwise, both IE1 and IE2 show a significant increase in the damage score for the cortex of renal tissue compared with (C-, E3, and E4). In contrast, a substantial increase ($P \geq 0.05$) in the damage score was observed in the medulla of IE1 compared with IE2. The tissue damage scores were divided into four categories (Minimal 0-10%, mild 10-20%, moderate 20- 30%, and severe 30 ≥) seen in the materials and methods in the Table.

Table: renal tissue damage scoring system criteria.

Score system criteria		
Grade	Necrosis percentage	Score
Minimal	0-10% of the cortex or medulla area	1
Mild	10-20% of the cortex or medulla area	2
Moderate	20-30% of the cortex or medulla area	3
Severe	> 30% of cortex or medulla area	4

In the cortex, the severe lesion was observed in (60%) of the C+ group rats and not in other IE1 and IE2-treated groups. Moderate cortex injury was observed in (40%) of C+ groups and (20%) of IE1 and was not observed in IE2. Mild cortex injury was observed in 60% of IE1 group rats and in (20%) of IE2 group rats. However, the mild grades of cortex injury were not observed in C+ group rats. The minimal grades of cortex injury were observed in (20%) of the IE1 group rats, and in (80%) of the IE2 group rats, mild grades of cortex injury were not observed in the C+ group rats (Figures -16 A).

In the medulla, the severe lesion was observed in (60%) of the C+ group rats and not observed in other groups IE1 and IE2-treated groups rats. Moderate grades of medulla injury were observed in (40%) of the C+ group rats, 20% of IE1 was not observed in other group IE2 treated groups rats, and mild grades of medulla injury were observed in (80%) of IE1 and were observed in (40%) of IE2. While not observed in C+ group rats. The minimal grades of medulla injury were observed in (60%) of IE2 group rats and did not appear in C+ and IE1 treated rats (Figures -16 B).

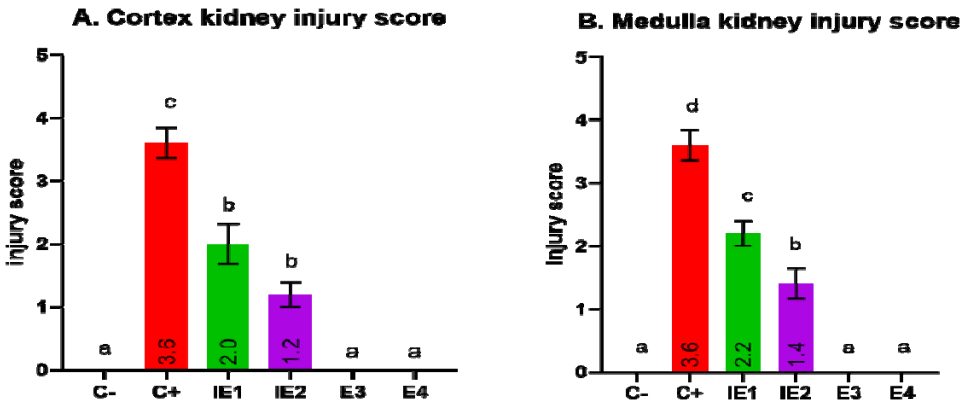

Figure (16 A and B): The tissue damage score values for renal tissue of rats. The graphs show the effect of eugenol and iron dextran on the cortex and medulla in the renal tissue. The different letters explained the significant differences among groups, while the similar letters denote non-significant differences among groups. The error bars explain mean ± SEM for p-value at ($p \geq 0.05$); ANOVA one-way statistical analysis was used to calculate the significance differences among groups.

Discussion

This study aimed to investigate the protective effects of eugenol against iron-induced nephrotoxicity in albino rats to explore biochemical, oxidative, and histopathological parameters to assess eugenol's impact on renal function. The anticipated benefits include a better understanding of eugenol's therapeutic potential and insights into potential preventive or complementary strategies for managing iron-induced renal.

The investigation into the role of eugenol against nephrotoxicity induced by iron overload in albino rats revealed noteworthy outcomes after a 30-day treatment period. Notably, the positive control group subjected to iron dextran injections exhibited a significant elevation in serum creatinine concentration, indicating iron-induced renal dysfunction. In contrast, groups

receiving eugenol alongside iron injection demonstrated no significant differences in serum creatinine levels compared to each other. This suggests a potential protective effect of eugenol against iron-induced nephrotoxicity. These results agree with previous studies on eugenol's antioxidant and anti-inflammatory properties, highlighting its potential to mitigate renal impairment caused by oxidative stress (Said, 2011; Fathy *et al*., 2022).

Generally, the mechanism influencing the role of eugenol on the level of creatinine involves its multifaceted antioxidant and anti-inflammatory properties on creatinine can explain by which as explain eugenol (Said, 2011; Asker *et al*., 2021; Fathy *et al*., 2022), known for its free radical scavenging abilities effectively mitigates oxidative stress and lipid peroxidation in the renal tissue that by eliminating electrons from free radicals and preventing Fe^{2+} oxidation by H_2O_2, eugenol inhibit radical (OH^{-}) production, ultimately suppressing lipid peroxidation, Additionally, as explained eugenol's anti-inflammatory actions include the modulation of cytokine levels by suppressing cyclooxygenase II and inhibiting cell proliferation. These combined effects contribute to reducing renal malondialdehyde levels, a marker of lipid peroxidation, and positively impact antioxidant defence mechanisms. While the exact pathways by which eugenol influences creatinine levels may involve a complex interplay of its antioxidant and anti-inflammatory actions, the overall outcome is a significant protective effect on renal function in the context of Iron overload syndrome-induced renal injury (Bachiega *et al*., 2012; Aboelwafa *et al*., 2022; Gharaei *et al*., 2022).

The blood urea nitrogen observed increase in the concentration in the control positive (C+) group is consistent with previous studies indicating iron's adverse effects on renal function (Ige *et al*., 2019). However, the significant decrease in BUN concentration in the IE1 group (iron dextran + eugenol 50 mg/kg) compared to other eugenol groups implies a potential dose-dependent protective effect of eugenol against iron-induced renal damage. This finding aligns with previous studies suggesting eugenol's capacity to ameliorate renal injury through its antioxidant and anti-inflammatory mechanisms (Said, 2011; Arase *et al*., 2020). Furthermore, the non-significant difference in blood urea nitrogen concentration between the IE1 group and the control negative group suggests that eugenol at a dose of 50 mg/kg may effectively counteract the iron-induced rise in blood urea nitrogen levels, bringing them closer to baseline levels (Gharaei *et al*., 2022).

The investigation into the effects of iron injection and oral eugenol on biochemical serum concentration parameters in male rats revealed significant alterations in serum reduced GSH and increased serum MDA. The GSH levels exhibited a notable decrease in the C+ group, indicative of oxidative stress induced by iron dextran injections, which eugenol treatment showed dose-dependent effects, with the IE2 group displaying significantly lower GSH compared to another group due to the antioxidant effect of eugenol (Barhoma, 2019; Sharma *et al*., 2019; Abdel-Magied *et al*., 2020).

In terms of MDA concentration, the C+ group demonstrated elevated levels, suggesting oxidative damage, while eugenol-treated groups displayed varied responses since the IE1 exhibited lower MDA than E3, E4, and IE2 showed comparable levels with E3 and E4; however, they had significantly lower MDA than both IE2 and E3. The control negative group displayed substantially lower MDA compared to all other groups. This study agreed with previous research indicating eugenol's potential antioxidant effects, as evidenced by GSH modulation, and its ability to mitigate lipid peroxidation, as reflected in MDA levels (Gharaei *et al*., 2022). In additionally, the dose-dependent responses emphasize the nuanced impact of eugenol on oxidative stress markers (Sharma *et al*., 2019) of its therapeutic potential in iron-induced renal injury, consistent with earlier anti-inflammatory and antioxidant properties (Mateen *et al*., 2019ab; Kumar *et al*., 2021; Fathy *et al*., 2022).

In terms of erythropoietin (EPO), it is a crucial hormone in the erythropoiesis regulatory cycle, which is produced by peritubular cells in the kidney; EPO responds to decreased oxygen delivery as hypoxia or elevated and acts on erythroid precursors, erythropoietin prevents apoptosis and enhances transferrin receptor expression, promoting increased red blood cell production. The augmented RBC count alleviates hypoxia, initiating a negative feedback loop that down-regulates hypoxia-inducible factor. Consequently, this increases hemoglobin levels, contributing to the intricate balance of the erythropoietin system (Hemani *et al*., 2021).

Examining serum erythropoietin concentration in male albino rats subjected to iron dextran injection and daily oral eugenol administration revealed significant variations in hematological parameters. As shown in the result of the C- group, erythropoietin is in the normal range in the everyday physiological context. However, in the context of the iron overload C+ group, where there is an excess of iron in the body, the relationship between erythropoietin levels and iron is more complex since the iron overload can lead to oxidative stress agents damage in

various tissues, including the kidneys, these agents can involve free superoxide radicals, hydrogen peroxide, singlet oxygen, nitric oxide (NO), and peroxynitrite (Maiese *et al*., 2008; Yun *et al*., 2020; Mohammad *et al*., 2021).

The Kidneys are central to erythropoietin production, and in the presence of iron overload-induced kidney damage, there can be an increase in erythropoietin production as a compensatory mechanism since the elevated erythropoietin levels in iron overload may be an attempt by the body to counteract the negative impact of iron-induced tissue damage, particularly in the kidneys, and to support the continued production of RBCs (Dang *et al*., 2010; Sun *et al*., 2018). The increased erythropoietin, in turn, stimulates the bone marrow to produce more RBCs. It contributes to an overall rise in RBC levels (Sun *et al*., 2018). Furthermore, it is noteworthy that EPO is primarily produced in the kidneys, with additional production and secretion occurring in the liver, brain, and uterus (Badi *et al*., 2022). Notably, EPO secretion in the brain seems to exhibit a more sustained pattern than in peripheral organs like the kidney, suggesting a potential origin of EPO production in the brain (Maiese *et al*., 2008).

This production may involve crossing the blood-brain barrier to reach the bloodstream and peripheral organs. In addition, hypoxia-inducible factor-la (HIF-1a) plays a pivotal role in the cellular response to hypoxia; the hypoxia-induced factor1 a controls the expression of EPO and EPOR during periods of reduced oxygen content. Prior studies have suggested that HlF-1a induces a reduction in intracellular reactive oxygen species (ROS) levels (Uchewa *et al*., 2023). Conversely, decreased levels of HlF-1a have been linked to elevated ROS levels, contributing to cell apoptosis in certain tumors. Furthermore, the activity of HlF-1a is influenced by the concentration of iron, a cofactor of prolyl hydroxylase domain 2 (PID2). PHD2 is the essential hydroxylase involved in oxygen sensing for HlF-1a. Excess iron impacts oxygen-sensing machinery, particularly concerning HIF-la. HIF-1a is a crucial sensing regulator that responds to low oxygen conditions, and iron availability modulates its activity (Z Abed Al-Kareem *et al*., 2022). Iron serves as a cofactor for PHD2, an essential enzyme responsible for the degradation of HIF-la. When iron is abundant, PHD2 is activated, leading to the degradation of HIF-la and, consequently, a decrease in EPO production. Conversely, under conditions of iron deficiency or low iron availability, reduced PHD2 activity allows HIF-la to accumulate, stimulating EPO production as a compensatory response to low oxygen levels (Zheng *et al*., 2017; Hu *et al*., 2020).

On the other hand, the serum erythropoietin levels exhibited a significant reduction in the iron-treated groups (IE1, IE2) compared to the control positive (C1) group, indicating a potential impact of iron overload on erythropoiesis. Interestingly, the E4 group, receiving high-dose eugenol, demonstrated the highest serum EPO levels among all groups. Suggesting a modulatory effect of eugenol on erythropoietin regulation, those investigating the hematopoietic and antioxidant effects of eugenol are essential to understand further the potential therapeutic implications of eugenol in iron-induced hematological alterations (Arab *et al*., 2018; Mateen *et al*., 2019ab; Fathy *et al*., 2022).

The Kidney Injury Molecule-1 (KIM-1) is a transmembrane glycoprotein expressed by proximal tubular cells and is recognized as an early, sensitive, and specific urinary biomarker for kidney injury. It has been associated with the severity of acute and chronic kidney damage. The ĶIM-1 acts as a phosphatidylserine phagocytosis and scavenger receptor, which binds to lipids on the surface of apoptotic and necrotic cells and oxidases LDL. Furthermore, it acts as a phagocytic receptor, helping engulf dead and necrotic debris in the injured epithelial tubules, thus transforming the epithelial cell into semi-professional phagocytes. The KIM-1 plays a critical role in the progression of kidney diseases and is used as a reliable biomarker for kidney injury. It has been found to correlate with the amount of acute tubular necrosis and interstitial fibrosis/ tubular atrophy (IF/ TA) on kidney biopsy and elevated KIM-1 predicted initial estimated glomerular filtration rate (Fazel *et al*., 2020).

KIM-1 also mediated fatty acid uptake by renal tubule cells to promote progressive diabetic kidney disease (Bonventre, 2009; Peng *et al*., 2020). The results of the study revealed significant findings concerning the impact of iron dextran injection and daily oral eugenol administration On KIM-I levels in male albino rats, which demonstrates a noteworthy increase in KIM-1 concentration in the C+ group compared to all experimental groups, as shown in previous studies (van Raaij *et al*., 2019) were illustrated that iron overload increased the KIM-1. Interestingly, the 1E2 group exhibited a notable decrease in KIM-1 levels compared to the IE1 and E4 groups while maintaining a non-significant difference with the E3 group. Moreover, no significant differences were observed among the eugenol-treated groups (IE1, E3, and E4) or between the C- and IE2 groups. These findings suggest a potential mitigating effect of eugenol, particularly at higher doses, on iron-induced elevation of KIM-1 levels (Aboelwafa *et al*., 2022; Kuang *et al*., 2023).

The present study showed in pathological examination that controls negative and eugenol-treated groups (E3 and E4) maintain unaltered kidney histology. Compared with the control positive (C+) group, induced with iron dextran injection, this causes renal damage characterized by necrosis in proximal and distal convoluted tubules, accompanied by inflammatory cell infiltration (Ganz, 2013; Teschke, 2022). Eugenol causes the potential antioxidant properties and observed effect, which counteract oxidative stress induced by iron overload. The iron dextran and eugenol-treated groups (IE1, IE2) exhibit standard histological architecture, reduced necrosis, and inflammatory cell infiltration compared to the control positive group. This suggests a protective effect of eugenol against iron-induced renal damage (Jaganathan and Supriyanto, 2012; Barhoma, 2019; Gharaei *et al*., 2022).

Notably, the Eugenol administration at varying dosages presents nuanced effects, with the IE1 group showing moderate necrosis and inflammatory cell aggregation. In contrast, the IE2 group showed restoration of normal architecture with mild inflammatory cell infiltration. These observations implicate iron overload-induced oxidative stress due to excessive iron in the kidney, leading to elevated iron levels contributing to the production of ROS. ROS induces damage to cellular components, including lipids, proteins, and DNA, leading to oxidative injury and subsequent inflammatory responses (Refaat *et al*., 2018; Baruah *et al*., 2023). Eugenol is known for its antioxidative properties, which are posited to mitigate oxidative stress, attenuate inflammatory reactions, and preserve renal tissue integrity (Adli *et al*., 2022). The dose-dependent impact of eugenol underscores the imperative for further investigations into the specific molecular pathways modulated by eugenol in the iron-induced histopathological alterations in the kidney (Toprak *et al*., 2022).

Conclusion

In conclusion, our findings suggest that eugenol exhibits nephroprotective effects against iron overload-induced nephrotoxicity, as evidenced by a reduction in kidney injury molecule-1 (Kim-1) concentration and mitigated renal tissue damage. Notably, the administration of eugenol at a dosage of 50 mg/kg body weight demonstrated superior efficacy in attenuating nephrotoxicity compared to the higher dosage of 100 mg/kg body weight. These results highlight the dose-dependent nature of eugenol's protective effects and underscore its potential as a therapeutic agent for the management of iron overload-induced renal injury. Further mechanistic studies are

warranted to elucidate the precise molecular pathways involved in eugenol-mediated nephroprotection.

Author Contributions

Both authors Ahmad M. Malik and Nabeel M. Naji designed and performed the experiment parameters, measured the serum blood parameter, collected the data, and analyzed also prepared the tissue slices and examined to be photographed using an optical microscope camera, wrote the manuscript and agreed to the published of the manuscript.

Funding

There is no funding entity for this research.

Conflict of interest

There is no conflict of interest**.**

References

Abdel-Magied, N., Elkady, A. A., and Abdel Fattah, S. M. (2020). Effect of low-level laser on some metals related to redox state and histological alterations in the liver and kidney of irradiated rats. *Biological trace element research.*, *194*(2), 410-422. https://doi.org/10.1007/s12011-019-01779-3. PMID: 31313245.

Abdul AL-Abbas, A. A. H., & Mlaghee, S. M. (2023). Therapeutic Effect of Curcumin on Dermatitis Induced by Acetone in Female Rats. *Kufa Journal for Veterinary Medical Sciences*., *14*(2). 1. https://doi.org/10.36326/kjvs/2023/v14i212138.

Aboelwafa, H. R., Ramadan, R. A., Ibraheim, S. S., and Yousef, H. N. (2022). Modulation Effects of Eugenol on Nephrotoxicity Triggered by Silver Nanoparticles in Adult Rats. *Biology*., *11*(12), 1719. https://doi.org/10.3390/biology11121719.

Adli, D. E. H., Ziani, K., Kourat, D., Brahmi, M., Souidi, S. A., Naar, A., ... and Slimani, M. (2022). Ameliorative Effect of The Essential Oil of Syzygium aromaticum in Wistars Rats Exposed to Aluminum Chloride. *Egyptian Academic Journal of Biological Sciences. C, Physiology and Molecular Biology*., *14*(2), 403-413. https://doi.org/10.21608/EAJBSC.2022.277234.

Alpert, A. J., and Gilbert, H. F. (1985). Detection of oxidized and reduced glutathione with a recycling postcolumn reaction. *Analytical biochemistry*., 144(2), 553-562. https://doi.org/10.1016/0003-2697(85)90153-8. PMID: 3993916.

Al-Sharafi, N. M., & Al-Sharafi, M. R. (2014). Study the effects of ginger (Zingiber officinale) extract on serum lipid in hypothyroidism male rats induce by propylthiouracil. *Kufa Journal for Veterinary Medical Sciences*., *5*(2), 258-266. https://doi.org/10.36326/kjvs/2014/v5i24185.

Arab, H. H., Salama, S. A., and Maghrabi, I. A. (2018). Camel milk ameliorates 5-fluorouracil-induced renal injury in rats: targeting MAPKs, NF-κB and PI3K/Akt/eNOS pathways. *Cellular Physiology and Biochemistry*., *46*(4), 1628-1642. https://doi.org/10.1159/000489210. PMID: 29694984.

Arase, H., Yamada, S., Hiyamuta, H., Taniguchi, M., Tokumoto, M., Tsuruya, K., ... and Kitazono, T. (2020). Modified creatinine index and risk for long-term infection-related mortality in hemodialysis patients: ten-year outcomes of the Q-Cohort Study. *Scientific reports*., *10*(1), 1241. https://doi.org/10.1038/s41598-020-58181-6. PMID: 31988325.

Asker, M. E., Ali, S. I., Mohamed, S. H., Abdelaleem, R. M., and Younis, N. N. (2021). The efficacy of bone marrow-derived mesenchymal stem cells and/or erythropoietin in

ameliorating kidney damage in gamma irradiated rats: Role of non-hematopoietic erythropoietin anti-apoptotic signaling. *Life Sciences*., *275*, 119388. https://doi.org/10.1016/j.lfs.2021.119388. PMID: 33774028.

Bachiega, T. F., de Sousa, J. P. B., Bastos, J. K., and Sforcin, J. M. (2012). Clove and eugenol in noncytotoxic concentrations exert immunomodulatory/anti-inflammatory action on cytokine production by murine macrophages. *Journal of Pharmacy and Pharmacology*, *64*(4), 610-616. https://doi.org/10.1111/j.20427158.2011.01440.x. PMID: 22420667.

Badi, N., Fazelipour, S., Naji, T., Babaei, M., and Kalantari Hesari, A. (2022). Histomorphometric and biochemical study of liver and thyroid hormones following administration of MoO3 nanoparticles in female rats. *Iranian Journal of Veterinary Medicine*, *16*(2), 188-201. https://doi.org/10.22059/IJVM.2021.330872.1005196.

Barhoma, R. A. E. (2019). The role of eugenol in the prevention of chromium-induced acute kidney injury in male albino rats. *Alexandria journal of medicine*, 54 (4), 711–715. https://doi.org/10.1016/j.ajme.2018.05.006.

Baruah, B., Tamuli, S. M., Begum, S. A., Dutta, B., Bora, D. P., Borah, B., ... and Tamuly, B. S. (2023). The effects of acute iron overload in wistar rats. *The Pharma Innovation Journal., 12* (12), 1394-1398. https://dx.doi.org/10.22271/tpi.

Bonventre, J. V. (2009). Kidney injury molecule-1 (KIM-1): a urinary biomarker and much more. *Nephrology Dialysis Transplantation*., *24*(11), 3265-3268. https://doi.org/10.1093/ndt/gfp010. PMID: 19318357.

Dable-Tupas, G., Tulika, V., Jain, V., Maheshwari, K., Brakad, D. D., Naresh, P. N., & Suruthimeenakshi, S. (2023). Bioactive compounds of nutrigenomic importance-11. In: *Role of nutrigenomics in modern-day healthcare and drug discovery*. Genevieve Dable-Tupas, Chukwuebuka Egbuna (eds). (2nd ed.) Elsevier. p. 301-342. https://doi.org/10.1016/B978-0-12-824412-8.00003-5. ISBN: 9780128244128.

Dang, J., Jia, R., Tu, Y., Xiao, S., and Ding, G. (2010). Erythropoietin prevents reactive oxygen species generation and renal tubular cell apoptosis at high glucose level. *Biomedicine and*

Pharmacotherapy, *64*(10), 681-685. https://doi.org/10.1016/j.biopha.2010.06.011. PMID: 20685070.

Elkhadragy, M. F., AQEEL, N. S. M. A., Yehia, H. M., Abdel-Gaber, R., & Hamed, S. S. (2022). Histological and molecular characterization of the protective effect of Eugenia caryophyllata against renal toxicity induced by vitamin D in male wistar rats. *Food Science and Technology.*, *42* (3), 1-9. https://doi.org/10.1590/fst.97522.

Fathy, M., Abdel-Latif, R., Abdelgwad, Y. M., Othman, O. A., Abdel-Razik, A. R. H., Dandekar, T., and Othman, E. M. (2022). Nephroprotective potential of eugenol in a rat experimental model of chronic kidney injury; targeting NOX, TGF-β, and Akt signaling. *Life Sciences.*, *308*, 120957. https://doi.org/10.1016/j.lfs.2022.120957. PMID: 36113730.

Fazel, M., Sarveazad, A., Ali, K. M., Yousefifard, M., and Hosseini, M. (2020). Accuracy of urine kidney injury molecule-1 in predicting acute kidney injury in children; a systematic review and meta-analysis. *Archives of academic emergency medicine.*, *8*(1). https://doi.org/10.22037/aaem.v8i1.584. PMID: 32309808.

Ganz, T. (2013). Systemic iron homeostasis. *Physiological reviews.*, *93*(4), 1721-1741. https://doi.org/10.1152/physrev.00008.2013. PMID: 24137020.

Gharaei, F. K., Lakzaei, H., Niazi, A. A., Jahantigh, M., Shahraki, M. R., & Safari, T. (2022). The protective effects of eugenol on metabolic syndrome, renal damages. *Journal of Renal Injury Prevention.*, *11*(1), 5. https://doi.org/10.34172/jrip.2022.04.

Hemani, S., Lane, O., Agarwal, S., Yu, S. P., and Woodbury, A. (2021). Systematic review of erythropoietin (EPO) for neuroprotection in human studies. *Neurochemical Research.*, *46*(4), 732-739. https://doi.org/10.1007/s11064-021-03242-z. PMID: 33521906.

Heriatmo, N. L., Estuningtyas, A., & Soetikno, V. (2023). Iron-Overload Conditions: Manifestations to the Kidney Organs–A Review. *Borneo Journal of Pharmacy.*, *6*(4), 360-369. https://doi.org/10.33084/bjop.v6i4.4411.

Hsu, C. C., Senussi, N. H., Fertrin, K. Y., & Kowdley, K. V. (2022). Iron overload disorders. *Hepatology communications*., *6*(8), 1842-1854. https://doi.org/10.1002/hep4.2012. PMID: 35699322.

Hu, J., Meng, F., Hu, X., Huang, L., Liu, H., Liu, Z., and Li, L. (2020). Iron overload regulate the cytokine of mesenchymal stromal cells through ROS/HIF-1α pathway in Myelodysplastic syndromes. *Leukemia Research*., *93*, 106354. https://doi.org/10.1016/j.leukres.2020.106354. PMID: 32380365.

Ige, A. O., Ongele, F. A., Adele, B. O., Emediong, I. E., Odetola, A. O., & Adewoye, E. O. (2019). Pathophysiology of iron overload-induced renal injury and dysfunction: Roles of renal oxidative stress and systemic inflammatory mediators. *Pathophysiology*, *26*(2), 175-180. https://doi.org/10.1016/j.pathophys.2019.03.002. PMID: 30910397.

Ikawati, S., Himawan, T., Abadi, A., Sarno, H., & Fajarudin, A. (2022). In silico study of eugenol and trans-caryophyllene also clove oil fumigant toxicity on Tribolium castaneum. *Journal of Tropical Life Science*., *12*(3), 339-349. https://doi.org/10.11594/jtls.12.03.07.

Jablonski, P., Howden, B. O., Rae, D. A., Birrell, C. S., Marshall, V. C., and Tange, J. (1983). An Experimental Model for Assessment of Renal Recovery from Warm Ischemia. *Transplantation.*, 35(3), 198–204. https://doi.org/10.1097/00007890-198303000-00002. PMID: 6340272.

Jaganathan, S. K., and Supriyanto, E. (2012). Antiproliferative and molecular mechanism of eugenol-induced apoptosis in cancer cells. *Molecules*., *17*(6), 6290-6304. https://doi.org/10.3390/molecules17066290. PMID: 22634840.

Jirkof, P., and Lofgren, J. (2023). Anesthesia and analgesia in laboratory rodents-14. In :Anesthesia and Analgesia in Laboratory Animals. Melissa C. Dyson, Paulin Jirkof, (eds). (3rd ed.). American College of Laboratory Animal Medicine, Academic Press. p. 287-356. https://doi.org/10.1016/B978-0-12-822215-7.00007-X. ISBN: 9780128222157.

Koohkan, O., Morovvati, H., and Mirghaed, A. T. (2023). Effects of Spirulina platensis on Iron Oxide Nanoparticles Induced-oxidative Stress and Liver Damage in Grey Mullet (Mugil cephalus). *Iranian Journal of Veterinary Medicine*, *17*(1). https://doi.org/10.22059/IJVM.17.1.1005284.

Kuang, B. C., Wang, Z. H., Hou, S. H., Zhang, J., Wang, M. Q., Zhang, J. S., ... and Gong, N. Q. (2023). Methyl eugenol protects the kidney from oxidative damage in mice by blocking the Nrf2 nuclear export signal through activation of the AMPK/GSK3β axis. *Acta Pharmacologica Sinica*., *44*(2), 367-380. https://doi.org/10.1038/s41401-022-00942-2. PMID: 35794373.

Kumar, A., Siddiqi, N. J., Alrashood, S. T., Khan, H. A., Dubey, A., & Sharma, B. (2021). Protective effect of eugenol on hepatic inflammation and oxidative stress induced by cadmium in male rats. *Biomedicine & Pharmacotherapy*., *139*, 111588. https://doi.org/10.1016/j.biopha.2021.111588. PMID: 33862491.

Luna, L. G. (1968). Manual of histologic staining methods of the Armed Forces Institute of Pathology. In: *Manual of histologic staining methods of the Armed Forces Institute of Pathology*. McGraw-Hill. (eds) (3rd ed.) New York. p. 258-1968. https://doi.org/10.29079/vol14iss2art34922.

Maiese, K., Chong, Z. Z., Hou, J., and Shang, Y. C. (2008). Erythropoietin and oxidative stress. *Current Neurovascular Research*., *5*(2), 125-142. https://doi.org/10.2174/156720208784310231. PMID: 18473829.

Mateen, S., Rehman, M. T., Shahzad, S., Naeem, S. S., Faizy, A. F., Khan, A. Q., ... and Moin, S. (2019a). Anti-oxidant and anti-inflammatory effects of cinnamaldehyde and eugenol on mononuclear cells of rheumatoid arthritis patients. *European journal of pharmacology*., *852*, 14-24. https://doi.org/10.1016/j.ejphar.2019.02.031.

Mateen, S., Shahzad, S., Ahmad, S., Naeem, S. S., Khalid, S., Akhtar, K., ... and Moin, S. (2019b). Cinnamaldehyde and eugenol attenuates collagen induced arthritis via reduction of free radicals and pro-inflammatory cytokines. *Phytomedicine*., *53*, 70-78. https://doi.org/10.1016/j.phymed.2018.09.004.

Melo, N. O. R., Silva, M. S., & Lima, W. P. (2023). Effect of eugenol and gum arabic on oxidative stress and genotoxicity in rat spleen, kidney and lung tissue following colorectal carcinogenesis. *International Journal of Herbal Medicine*., *11* (1), 22-9. https://doi.org/10.22271/flora.2023.v11.i1a.849.

Mohammad, G., Matakidou, A., Robbins, P. A., and Lakhal-Littleton, S. (2021). The kidney hepcidin/ferroportin axis controls iron reabsorption and determines the magnitude of kidney and systemic iron overload. *Kidney international*., *100*(3), 559-569. https://doi.org/10.1016/j.kint.2021.04.034. PMID: 33991530.

Ntumi, S. (2021). Reporting and interpreting One-Way Analysis of Variance (ANOVA) using a data-driven example: A practical guide for social science researchers. *Journal of Research in Educational Sciences*., *12*(14), 38-47. https://doi.org/10.14505/jres.v12.14.04.

Peng, S., Liu, N., Wei, K., Li, G., Zou, Z., Liu, T., and Lin, Y. (2022). The predicted value of kidney injury molecule-1 (KIM-1) in healthy people. *International Journal of General Medicine*., 15, 4495-4503. https://doi.org/10.2147/IJGM.S361468. PMID: 35518515.

Polaka, S., Nalla, L. V., Kalpeshkumar, R. D., Teja, P. S., More, A., Tekade, M., ... & Tekade, R. K. (2023). Drug-induced nephrotoxicity and its biomarkers. In: *Essentials of Pharmatoxicology in Drug Research*. Rakesh Tekade (eds). Academic Press. *1*, p. 289-316. https://doi.org/10.1016/B978-0-443-15840-7.00011-7. ISBN: 9780443158407.

Refaat, B., Abdelghany, A. H., BaSalamah, M. A., El-Boshy, M., Ahmad, J., and Idris, S. (2018). Acute and chronic iron overloading differentially modulates the expression of cellular iron-homeostatic molecules in normal rat kidney. *Journal of Histochemistry and Cytochemistry*., *66*(11), 825-839. https://doi.org/10.1369/0022155418782696. PMID: 29873589.

Rifai, N. (2022). Tietz textbook of laboratory medicine. Nader Rifai (eds). (7th ed.) Elsevier Health Sciences. p.1584. ISBN: 9780323834674.

Ríos-Silva, M., Cárdenas, Y., Ortega-Macías, A. G., Trujillo, X., Murillo-Zamora, E., Mendoza-Cano, O., ... & Huerta, M. (2023). Animal models of kidney iron overload and

ferroptosis: a review of the literature. *BioMetals*., *36*(6), 1173-1187. https://doi.org/10.1007/s10534-023-00518-5. PMID: 37356039.

Said, M. M. (2011). The protective effect of eugenol against gentamicin-induced nephrotoxicity and oxidative damage in rat kidney. *Fundamental and clinical pharmacology*., *25*(6), 708-716. https://doi.org/10.1111/j.1472-8206.2010.00900.x.

saleh mehdy Al-zeiny, S., & Abbas, D. A. (2017). Comparative histological study of protective effect of oil and alcoholic extracts of dry palm dates and leaves (Phoenix dactylifera L) against CCL4 induced oxidative stress in rats. *Kufa Journal For Veterinary Medical Sciences*., *8*(1), 79-89. https://doi.org/10.36326/kjvs/2017/v8i14318.

Sales, G. T. M., & Foresto, R. D. (2020). Drug-induced nephrotoxicity. *Revista da Associação Médica Brasileira*., *66* (1), 82-90. https://doi.org/10.1590/1806-9282.66.S1.82**.** PMID: 31939540.

Seyednejad, S. F., Shirani, D., Bokai, S., and Nasiri, S. M. (2023). Evaluation of Iron Status in Cats With Hypertrophic Cardiomyopathy With and Without Congestive Heart Failure. *Iranian Journal of Veterinary Medicine*, *17*(3), 209-216. https://doi.org/10.32598/IJVM.17.3.1005245.

Shahsavari, M., Norouzi, P., Kalalianmoghaddam, H., and Teimouri, M. (2023). Effects of Kudzu Root on Oxidative Stress and Inflammation in Streptozotocin-induced Diabetic Rats. *Iranian Journal of Veterinary Medicine*, *17*(4), 401-408. https://doi.org/10.32598/IJVM.17.4.1005281.

Sharma, U. K., Kumar, R., Gupta, A., Ganguly, R., Singh, A. K., Ojha, A. K., and Pandey, A. K. (2019). Ameliorating efficacy of eugenol against metanil yellow induced toxicity in albino Wistar rats. *Food and Chemical Toxicology*., *126*, 34-40. https://doi.org/10.1016/j.fct.2019.01.032. PMID: 30738991.

Sharma, V., & Singh, T. G. (2023). Drug induced nephrotoxicity-A mechanistic approach. *Molecular Biology Reports*., *50*(8), 6975-6986. https://doi.org/10.1007/s11033-023-08573-4. PMID: 37378746.

Spitz, D. R., and Oberley, L. W. (1989). An assay for superoxide dismutase activity in mammalian tissue homogenates. *Analytical biochemistry*., 179(1), 8-18. https://doi.org/10.1016/0003-2697(89)90192-9. PMID: 2547324.

Sun, Y., Liu, G., Jiang, Y., Wang, H., Xiao, H., and Guan, G. (2018). Erythropoietin Protects Erythrocytes Against Oxidative Stress-Induced Eryptosis In Vitro. *Clinical laboratory*., *64*(3), 365-369. https://doi.org/10.7754/Clin.Lab.2017.170924. PMID: 29739123.

Teschke, R. (2022). Aluminum, arsenic, beryllium, cadmium, chromium, cobalt, copper, iron, lead, mercury, molybdenum, nickel, platinum, thallium, titanium, vanadium, and zinc: molecular aspects in experimental liver injury. *International Journal of Molecular Sciences*., *23*(20), 12213. https://doi.org/10.3390/ijms232012213. PMID: 36293069.

Toprak, T., Sekerci, C. A., Aydın, H. R., Ramazanoglu, M. A., Arslan, F. D., Basok, B. I., ... & Tanıdır, Y. (2020). Protective effect of chlorogenic acid on renal ischemia/reperfusion injury in rats. *Archivio Italiano di Urologia e Andrologia*., *92*(2). 153-157. https://doi.org/10.4081/aiua.2020.2.153. PMID: 32597123.

Udani, K., Chris-Olaiya, A., Ohadugha, C., Malik, A., Sansbury, J., & Paari, D. (2021). Cardiovascular manifestations in hospitalized patients with hemochromatosis in the United States. *International Journal of Cardiology*., *342*, 117-124. https://doi.org/10.1016/j.ijcard.2021.07.060. PMID: 34343533.

Uchewa ,O. O. Chukwuemelie, C. E., Oviosun, A. I., and Ibegbu, A. O. (2023). Alleviating Effects of Clove Essential Oil Disolved in Dimethyl Sulfoxide (Dmso) Against Cadmium-Induced Testicular and Epididymal Damages in Male Wistar Rats. *Archives of Razi Institute*, *78*(6), 1728-1737. https:// doi.org/10.32592/ARI.2023.78.6.1728.

van Raaij, S. E., Rennings, A. J., Biemond, B. J., Schols, S. E., Wiegerinck, E. T., Roelofs, H. M., ... and van Swelm, R. P. (2019). Iron handling by the human kidney: Glomerular filtration and tubular reabsorption both contribute to urinary iron excretion. *American Journal of Physiology-Renal Physiology*., *316*(3), 606-614. https://doi.org/10.1152/ajprenal.00425.2018. PMID: 30623722.

Verna, F. D., & Estuningtyas, A. (2022). Hematological Profile of Iron Overload in Rats Administered with Fruit Extract of Mahkota Dewa (Phaleria macrocarpa). *Jurnal Farmasi Galenika (Galenika Journal of Pharmacy)(e-Journal)*., *8*(2), 117-123. https://doi.org/10.22487/j24428744.2022.v8.i2.15936.

Vilela, A. P., Ferreira, L., Biscaia, P. B., Silva, K. L. D., Beltrame, F. L., Camargo, G. D. A., ... & Farago, P. V. (2023). Preparation, Characterization and Stability Study of Eugenol-Loaded Eudragit RS100 Nanocapsules for Dental Sensitivity Reduction. *Brazilian Archives of Biology and Technology*., *66*, e23230300. https://doi.org/10.1590/1678-4324-ssbfar-2023230300.

Wu, A. H. (2006). Tietz Clinical Guide to Laboratory Tests-E-Book. Tietz Clinical Guide to Laboratory Tests-E-Book. Alan H.B., WU. (eds). (4th ed.) WB. Saunders Company, Elsevier Health Sciences. P. 1856.

Yun, S., Chu, D., He, X., Zhang, W., and Feng, C. (2020). Protective effects of grape seed proanthocyanidins against iron overload-induced renal oxidative damage in rats. *Journal of Trace Elements in Medicine and Biology*., *57*, 126407. https://doi.org/10.1016/j.jtemb.2019.126407. PMID: 31570250.

Z Abed Al-Kareem; N. D Aziz and M Ali Zghair. (2022). Hepatoprotective Effect of Coenzyme Q10 in Rats with Diclofenac Toxicity. *Archives of Razi Institute* 77, (2), 599-605. https://dio. org/10.22092/ARI.2022.357210.1998.

Zheng, Q. Q., Zhao, Y. S., Guo, J., Song, L. X., Fei, C. M., Zhang, Z., ... and Chang, C. K. (2017). Iron overload promotes erythroid apoptosis through regulating HIF-1a/ROS signaling pathway in patients with myelodysplastic syndrome. *Leukemia Research*, *58*, 55-62. https://doi.org/10.1016/j.leukres.2017.04.005. PMID: 28460338.